Electronic properties of expanded cesium

P. J. Kelly* and D. Glötzel
Max-Planck-Institut für Festkörperforschung, Heisenbergstrasse 1, D-7000 Stuttgart 80, Federal Republic of Germany
(Received 13 November 1985)

We present the results of an extensive series of self-consistent calculations for cesium between the equilibrium atomic volume and the critical density. Paramagnetic, ferromagnetic, and antiferromagnetic ordering on bcc, sc, and diamond lattices are considered. We find that, for all three lattices, antiferromagnetic ordering occurs before ferromagnetic ordering. In all cases, a metal-insulator transition occurs at a density ρ_{MI} lower than the density at which magnetic ordering occurs. There is a considerable spread in the values of ρ_{MI} for the different structures clustered about the experimental critical density $\rho_c = 0.41$ g/cm^3. Calculated electron densities at the nucleus do not, however, reproduce the experimentally observed trend even when a restricted dimerization of the structure is taken into account.

I. INTRODUCTION

The system proposed by Mott[1] in his original discussion of the metal-insulator transition was a lattice of hydrogen atoms with a half-filled band at high densities. The metal-insulator (M-I) transition occurs when the density of the system is decreased and the bandwidth becomes comparable to the Coulomb energy associated with multiple occupancy of a single site. This system, however, cannot be realized in practice. A closely related system is the liquid alkali metals which, expanded by heating, have recently been examined in detail. In particular, liquid cesium has been investigated[2] from its normal melting point ($\rho_m \sim 1.83$ g/cm^3) to a density close to its critical density ($\rho_c = 0.41$ g/cm^3) corresponding to a volume change of more than a factor of 4. Measurements of the electrical transport properties[2] indicated that the M-I transition is associated with the gas-liquid critical point. In a study of the magnetic properties of expanded fluid cesium, Freyland[3] found that the uniform static mass susceptibility first decreases slightly and then rises rapidly by almost a factor of 5 with a maximum at a density almost double the critical density. This maximum was demonstrated by Warren[4] to be due to Curie-law limitation of the susceptibility at the high temperatures required at low density. From NMR measurements on liquid Cs El-Hanany *et al.*[5] confirmed the enhancement of the mass susceptibility and in addition concluded that there was a strong change in the q dependence of the susceptibility with decreasing density. By combining Freylands measurements of $\chi'(0,0)$ with their measurements of the Knight shift $\sim \langle |\psi(0)|^2 \rangle_{E_F} \chi'(0,0)$, Warren *et al.*[6] found that the Fermi electron charge density at the Cs nucleus $\langle |\psi(0)|^2 \rangle_{E_F}$ *decreased* with decreasing density rather than increasing towards the limiting atomic value. Similar results have also been obtained for Na.[7]

The ground-state properties of the correlated system described by Mott should, in principle, be described correctly by density-functional (DF) theory.[8,9] Rose and co-workers have investigated how well the local-spin-density (LSD) approximation[10,11] describes the M-I transition on a lattice of hydrogen atoms[12,13] and discussed applications to the dilute alkali-metal system.[14] Kelly *et al.*[15] have examined the M-I transition of a lattice of hydrogen atoms within the LSD approximation in detail, and without making any severe approximations such as the Wigner-Seitz[13,14] or tight-binding[12] approximations in order to solve the effective one-particle Schrödinger equation.[8] The conclusion of these studies was that, apart from inaccuracies in describing the actual M-I transition, the LSD approximation gave results which were very reasonable and in agreement with the limited results available from other methods.

In a system such as the liquid alkali metals, the effect of disorder should not be negligible, and indeed attempts focusing on the disorder have been made[16] to explain their low-density properties. In order to examine the predictions of the local-density approximation we neglect the effect of disorder. Although the experiments on liquid cesium have been performed between the normal melting point ($T_m = 29$ °C) and the critical point ($T_c = 1740$ °C, $P_c = 114$ bars, $\rho_c = 0.41$ g/cm^3), there are some indications for believing that the effects of temperature and disorder are of secondary importance for its electronic properties. For crystalline Cs the large value of the susceptibility enhancement is mainly due to the proximity of the Fermi level to a van Hove singularity in the density of states. Nevertheless, on melting there is only a small change of a few percent in the susceptibility.[3] Similarly, the volume derivative of the Knight shift for liquid Cs $(\partial \ln K / \partial \ln V)_T$ is, to within the experimental error bar, equal to that for crystalline Cs.[5] This indicates that long-range order does not dominate the electronic structure.

That temperature effects are not dominant is evidenced by the fact that the isothermal and isobaric variations of the Knight shift, $(\partial \ln K / \partial \ln \rho)_T$ and $(\partial \ln K / \partial \ln \rho)_P$, respectively, are the same to within the experimental accuracy.[5] The change in the Knight shift is primarily determined by change in the density.

One simple model for the structure of liquid Cs which we will consider is based on the following. A neutron dif-

fraction determination of the static structure factor[17] of expanded liquid rubidium indicates that as the density is reduced the nearest-neighbor distance d_{NN} remains approximately constant while the number of nearest neighbors decreases linearly with density. As in a recent paper by Warren and Mattheiss,[18] we model this by examining structures with different coordination number. The implicit assumption here is that the electronic properties are dominated by the local structure. In addition, we consider the effects of changing the interatomic separation and allow our system to order magnetically.

We find that this model does not predict an enhancement of the uniform static susceptibility such as one obtains for a fixed structure with variable nearest-neighbor separation. It does predict a change in the q dependence of the susceptibility. For all three crystal structures we have examined, an antiferromagnetic (AF) transition occurs at a higher density than the ferromagnetic (F) transition. The M-I transition occurs for densities $\rho < 0.60$ g/cm^3. We also calculate the Fermi electron charge density at the nucleus and find that it always increases towards the atomic limit with decreasing density in disagreement with experiment. Calculations where we allowed for a pairing of Cs atoms do not change this result.

II. METHOD OF CALCULATION

The electronic structure was determined self-consistently using the linear muffin-tin-orbital (LMTO) method.[19] A frozen core approximation was used and relativistic shifts were included using a scalar-relativistic procedure.[20] In the **k**-space summation[21] to determine densities of states (DOS), as many as 969 **k** points in the irreducible part of the Brillouin zone were used for the spin-polarized calculations where the magnetic moment converges particularly slowly. In the angular momentum expansion, terms with $l \leq 2$ were included. Inclusion of terms with $l=3$ resulted in very minor differences. Where necessary, we included the so-called combined correction terms[19] which correct for the finite number of terms in the angular momentum expansion and for the nonspherical shape of the Wigner-Seitz cell. In the case of structures with low coordination such as simple cubic (sc) and diamond structures we include additional "empty spheres" for more flexibility in describing the charge density.[22] To carry out spin-polarized calculations we used the parametrization of von Barth and Hedin.[10] For a detailed discussion of the local-spin-density description of the M-I transition as well as for more technical details see Ref. 15.

When the density of liquid Rb decreases by a factor of 2 from the normal melting point, the nearest-neighbor separation increases by only 4%. Over the same range the number of nearest-neighbor atoms decreases linearly.[17] Assuming a similar behavior holds for liquid Cs, we consider three simple crystal structures with different coordination, bcc, simple cubic, and diamond with 8, 6, and 4 neighbors, respectively. The AF ordering we consider is illustrated in Fig. 1. Considering the spin-up and spin-down atoms as different "chemical" species means that bcc→CsCl, sc→NaCl, and diamond→ZnS crystal structures.

To calculate the Fermi electron density at the nucleus $\langle |\psi(0)|^2 \rangle_{E_F}$ with the LMTO method is straightforward. It is given by

$$\langle |\psi(0)|^2 \rangle_{E_F} = \frac{N_s(E_F)}{N(E_F)} \frac{\phi_s^2(E_F,0)}{4\pi} \equiv \xi |\psi(0)|^2_{\text{atom}} , \quad (1)$$

where $N_l(E)$ is the l-projected spin-density of states,

$$N(E) = \sum_{l=0}^{l_{\max}} N_l(E) ,$$

and $2\int^{E_F} N(E)dE$ is the total number of electrons. $\phi_l(E,r)$ is the solution of the appropriate radial Schrödinger equation with energy E and is normalized so that

$$\int_0^S \phi_l^2(E,r) r^2 dr = 1 ,$$

where S is the radius of the Wigner-Seitz sphere which for a monatomic solid has the same volume as the Wigner-Seitz cell. Because of the weak (although integrable) divergence of $\phi_s(E,r)$ as $r \to 0$, for a point nucleus we take a point r_n close to the nucleus. For a recent discussion of this point as well as further references see Ref. 23. The results are insensitive to the choice of r_n. To simulate the smearing out of the density of states at high temperature, Eq. (1) is averaged over the energy range $E_F \pm kT$. Again, the results are not sensitive to this averaging.

At lower densities it has been suggested[3] that the Cs atoms will eventually pair. To investigate the effect this might have on $\langle |\psi(0)|^2 \rangle_{E_F}$ we consider dimerized structures derived from the bcc and diamond structures by allowing the neighboring atoms to pair along the $\langle 111 \rangle$ direction. This reduces the symmetry and requires integration over a larger irreducible Brillouin zone.

III. RESULTS

A. Uniform susceptibility

Within the LSD approximation the uniform spin susceptibility for an itinerant electron system has been shown[24–27] to have the enhanced form

$$\chi = \frac{\chi_0}{1 - N(E_F)I} , \quad (2)$$

where $\chi_0 = 2\mu_B^2 N(E_F)$ is the susceptibility for noninteract-

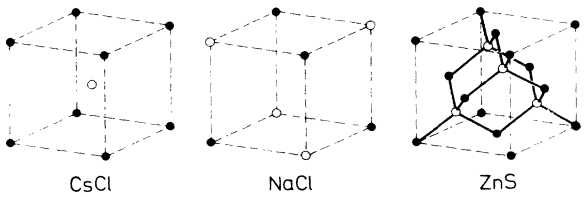

FIG. 1. Crystal structures used in the calculations, (a) CsCl, (b) NaCl, and (c) ZnS, which become the bcc, sc, and diamond structures, respectively, when all atom types are the same. The AF structures considered result from replacing the open (solid) circles with up (down) spins.

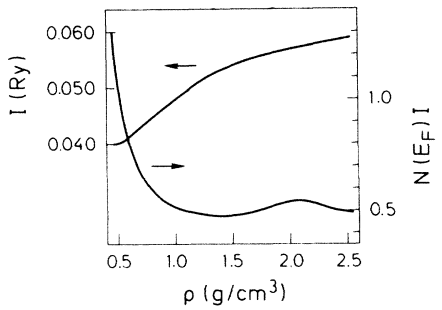

FIG. 2. Stoner parameter I and the product $N(E_F)I$ as a function of density for bcc Cs.

ing electrons. We evaluate the Stoner parameter I according to Ref. 26. It is essentially structure independent and changes only slowly with volume (Fig. 2). From a value of 57 mRy at $\rho=2.0$ g/cm^3 it decreases monotonically to a value of 40 mRy at $\rho=0.5$ g/cm^3.

In Table I we compare calculated values of I for H, Li, Na, K, Rb, and Cs. R_s is the Wigner-Seitz radius as determined by $4\pi R_s^3/3=$ volume per atom. We use rydberg atomic units throughout. For H, I was evaluated at the theoretical equilibrium lattice parameter.[15] I decreases with increasing atomic number as a result of the overall increase in the charge density.[27] The values given in Table I are essentially the same as those obtained in Ref. 26 where the same exchange-correlation potential[10] was used. They are approximately 20% smaller than those given by Janak who used a slightly different potential.[27] For all the alkalis except cesium we obtain values for $N(E_F)$ very similar to Janak[27] and Vosko *et al.*,[26] and the agreement of the calculated values of $\chi/\chi_{\rm FE}$, also given in Table I, with experiment is very good. $\chi_{\rm FE}$ is the free-electron susceptibility $2\mu_B^2 N_{\rm FE}(E_F)$.

In the case of Cs the calculated value of $\chi/\chi_{\rm FE}$ is 50% larger than the experimental value. Since I is the same as in Ref. 26, the difference must be attributed to differences in the evaluation of $N(E_F)$. From Fig. 3(a) it can be seen that the Fermi level lies very close to a van Hove singularity where the Fermi surface touches the Brillouin zone boundary at N. $N(E_F)$ is then very sensitive to the details of the band-structure calculation. The value for $N(E_F)$ in Ref. 26 calculated with spherical bands is therefore probably an underestimate and the good agreement with experiment must be regarded as fortuitous. In a recent self-consistent linearized augmented plane-wave (LAPW) calculation with a different exchange-correlation potential Warren and Mattheiss[18] find $N(E_F)=10.7$ states/Ry spin, somewhat larger than our value. The discrepancy here is probably due to their coarse mesh in **k** space. In an earlier study Jan *et al.*[28] found that the LD approximation resulted in a Fermi surface for Cs whose departure from an ideal spherical shape was too large compared with experiment. By adjusting the individual bands (equivalent to the introduction of a nonlocal potential) to obtain good agreement for the Fermi surface they simultaneously obtained a value for $N(E_F)$ of 7.53 states/Ry spin. Using this with our value of I in Eq. (2), we obtain a value of $\chi/\chi_0=2.04$ in very satisfactory agreement with experiment. It thus appears that the LSD approximation is not sufficiently accurate to yield precise absolute values of χ. In the following where we will be concerned with qualitative predictions of trends as a function of volume and structure this should be borne in mind.

The susceptibility calculated for bcc, sc, and diamond lattices of Cs using Eq. (2) is shown in Fig. 4. Also shown in Fig. 4 is the electron paramagnetic susceptibility for expanded liquid Cs extracted by Freyland[3] from the measured susceptibility by subtracting the Cs^+-ion core susceptibility and a correction for the orbital diamagnetic susceptibility of the conduction electrons. On melting there is only a small change of a few percent in the susceptibility.[3] This indicates that even though the Fermi level lies close to a van Hove singularity in bcc metallic Cs [Fig. 3(a)] the loss of long-range order is not critical for the value of $N(E_F)$. We note, however, that this method of extracting the paramagnetic susceptibility can involve a significant error because of uncertainties in our knowledge of the subtracted quantities. If we compare the value of $\chi(\rho_M)=0.61\times10^{-6}$ cm^{3}g^{-1} from Fig. 4 with the accurate value for χ of 0.49×10^{-6} cm^{3}g^{-1} derived from de Haas–van Alphen measurements on the perfect crystal at low temperature (Table I) we see that there is a discrepancy of about 20%. Here ρ_M is the nor-

TABLE I. Comparison of calculated values of χ for the bcc structure with experimental values. Both are normalized by the free-electron susceptibility $\chi_{\rm FE}$.

	R_s	I (Ry)	$N(E_F)$[a]	$\chi/\chi_{\rm FE}$ (Calc.)	$\chi/\chi_{\rm FE}$ (Expt.)
H	1.67	0.374	0.68	1.60	
Li	3.25	0.139	3.22	2.70	2.50[b]
Na	3.93	0.106	3.11	1.47	1.63[c]
K	4.86	0.076	4.99	1.67	1.70[d]
Rb	5.20	0.067	5.82	1.73	1.72[d]
Cs	5.63	0.057	9.54	3.24	2.14[e]

[a]In units of states/Ry atom spin.
[b]T. Kushida, J. C. Murphy, and M. Hanabusa, Solid State Commun. **15**, 1217 (1974).
[c]J. M. Perz and D. Shoenberg, J. Low Temp. Phys. **25**, 275 (1976).
[d]B. Knecht, J. Low Temp. Phys. **21**, 619 (1975).
[e]M. Springford, I. M. Templeton, and P. T. Coleridge, J. Low Temp. Phys. **53**, 563 (1983).

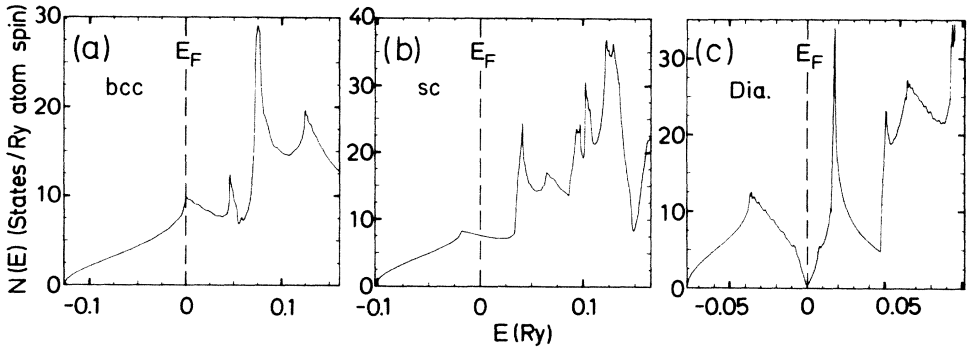

FIG. 3. Total DOS, $N(E_F)$, for (a) bcc, (b) sc, and (c) diamond structures. The curves shown were calculated at densities corresponding to $d_{NN}=10.03$ a.u.

mal low-temperature metal density, 1.997 g/cm^3.

Further decrease in the density leads to a shallow minimum at $\rho\approx 1.5$ g/cm^3, followed by a sharp increase to a maximum at $\rho=0.8$ g/cm^3, and then a decrease towards the critical density $\rho_c=0.41$ g/cm^3. It was recently pointed out by Warren[4] that at the increasing temperatures required to achieve lower densities the decrease in χ corresponds to the Curie-law limit of the free-spin susceptibility. While temperature effects can, in principle, be included in DF calculations, a straightforward application is known to lead to a serious overestimate of the Curie temperature.[24] In the remainder of this section we concentrate on the LSD description of χ between the density at the melting point, $\rho_m=1.83$ g/cm^3, and $\rho=0.8$ g/cm^3.

The first simple model we consider approximates the liquid of decreasing density by a series of structures with constant nearest-neighbor separation d_{NN} and decreasing number of nearest neighbors. We take $d_{NN}=10.03$ a.u., the value determined by neutron-diffraction[29] studies on liquid Cs at a temperature just above the melting point. For the bcc, sc, and diamond structures we consider, this corresponds to densities of 1.92, 1.47, and 0.96 g/cm^3, respectively, which are indicated by vertical arrows in Fig. 4. The susceptibilities calculated at these densities are shown joined by a dotted line. There is no evidence for an increase in the susceptibility. On the contrary, χ decreases monotonically to a near-zero value for the diamond structure at all densities. The reason for this is apparent in Fig. 3(c), where the Fermi level is seen to lie in a region of very low state density between the bonding and antibonding bands of the two atoms per unit cell in the diamond structure and is an artifact of the model. This has been pointed out independently by Warren and Mattheiss,[18] whose results are essentially the same as ours. They considered an additional structure with fourfold coordination which does not have a pseudogap at the Fermi level. This structure, however, also failed to reproduce the observed enhancement of the susceptibility.

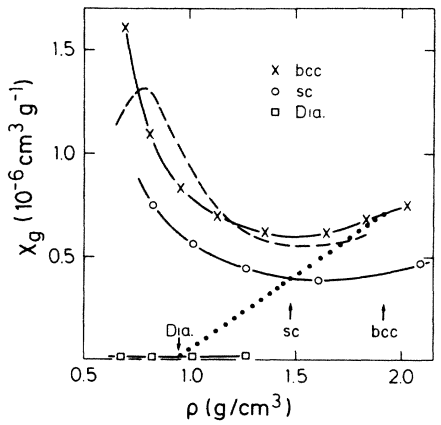

FIG. 4. Density dependence of the uniform static mass susceptibility, χ_g, calculated for the bcc, sc, and diamond structures. The dashed line is the paramagnetic susceptibility extracted from experiment by Freyland (Ref. 3). The dotted line corresponds to the sequence bcc-sc-diamond with $d_{NN}=10.03$ a.u.

Both χ_{bcc} and χ_{sc} exhibit a substantial enhancement with decreasing density. For a particular structure the mechanism is straightforward. $N(E_F)$ in Eq. (2) is inversely proportional to the bandwidth W which decreases as the interatomic separation d_{NN} increases. Even though a substantial uncertainty enters because of the sensitivity of $N(E_F)$ to the nearby van Hove singularity in the bcc structure mentioned previously, we might ask whether the decrease in the bandwidth is sufficient to explain the observed ratio $\chi(\rho=0.8)/\chi(\rho=1.83)=2.13$. Here ρ is in units of g/cm^3. By comparison, $\chi_{bcc}(\rho=0.8)/\chi_{bcc}(\rho=1.83)=1.6$ is considerably too small.

We can examine the effect of the decreasing bandwidth in the following way. For a rectangular DOS the bandwidth W is simply related to the second moment of the DOS, $\langle\Delta E^2\rangle$, by $W^2=12\langle\Delta E^2\rangle$. We use this to define an effective bandwidth for the real $N(E)$ by calculating the second moment,

$$\langle\Delta E^2\rangle=\frac{4\int^{E_F}N(E)(E-\bar{E})^2dE}{\int^{E_F}N(E)dE} \quad (3)$$

where

$$\bar{E}=\frac{\int^{E_F}N(E)E\,dE}{\int^{E_F}N(E)dE}\,.$$

Here E_F is the Fermi level corresponding to one valence electron per atom and the integral is over the occupied

band states. The bandwidths determined from the moments calculated with the actual $N(E)$ for the three structures are shown in Fig. 5. There are significant differences in the volume dependence of W for the different structures. At higher densities the smaller nearest-neighbor spacing in the lower coordination structure dominates and the diamond structure has the larger bandwidth. Even at densities as low as those shown in Fig. 5 we find that the higher coordination (larger d_{NN} for a given density) structure has the larger bandwidth. This indicates that the extreme tight-binding limit, where the hopping integral depends exponentially on d_{NN} and next-nearest-neighbor hopping is negligible, has not yet been reached. For a structural sequence with decreasing coordination on reducing the density it also implies an increase in $N(E_F)$ over and above what would be expected for a single structure. For a structureless DOS with $N(E_F)=1/W$, $\chi_{dia}(\rho=0.8)/\chi_{bcc}(\rho=1.83)=2.94$ where W has been taken from Fig. 5. However, close to ρ_m, $N(E_F)$ is dominated by structure in the DOS even in the liquid phase. We should take the experimental value for $\chi(\rho=1.83)\sim(0.5\text{–}0.6)\times10^{-6}$ cm^3 g^{-1} which reduces the density enhancement to ~ 1.3.

The structural model for Cs is based on the assumption that it behaves like Rb when expanded. We can use the results of our $T=0$ K calculations to see whether there are any significant differences in the electronic contribution to the total energies of Rb and Cs. The results of these calculations are shown in Fig. 6, where in both cases the density has been normalized to the normal metal density ρ_M. There are no apparent differences. No significance should be attached to the fact that there is no density where the sc structure has the lowest energy since it is the Gibbs free energy which determines which structure is favored.

Finally, we consider the mechanism responsible for the initial decrease in χ. Warren and Mattheiss[18] proposed that it was due to a narrowing of the d band caused by the reduction in coordination number. It can be seen from Fig. 4 that, even for a fixed coordination and changing interatomic spacing d_{NN}, there is a decrease in χ_{bcc} and χ_{sc}

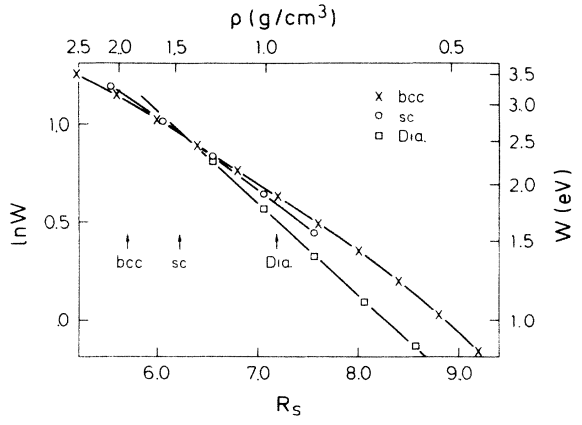

FIG. 5. Effective bandwidths W calculated from the second moment of the DOS as described in the text as a function of density. The vertical arrows indicate the densities for which $d_{NN}=10.03$ a.u. for the given structure.

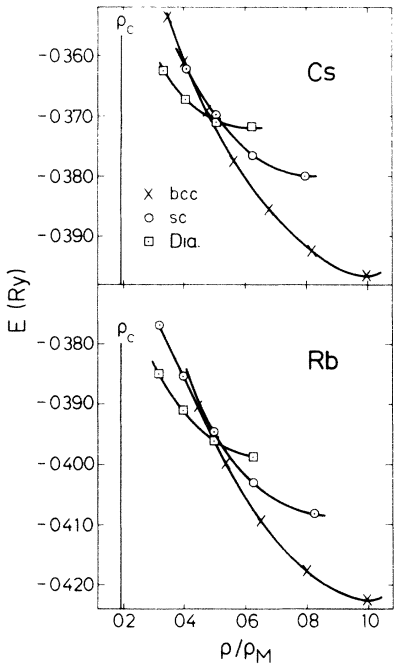

FIG. 6. Total energy (to within a constant) as a function of density for bcc, sc, and diamond structured Rb and Cs.

which matches the experimental decrease quite well. A simple model of a fixed I and increasing $N(E_F)$, however, predicts a monotonic increase in χ. It was suggested by Freyland[3] that a decrease in I with density might explain the initial decrease in χ. While I, as seen in Fig. 2, does indeed decrease with density, the effect is too small to account for the observed decrease. Instead, the decrease is caused by $N(E_F)$, which, as shown in Fig. 7, initially decreases when the volume is reduced.

There are two effects which we must consider. We start with a pure d band centered at ε_d and a pure s band centered at ε_s which overlap slightly. This is illustrated schematically in Fig. 8(a). When the interaction between them is switched on the two bands repel. This effect is strongest at the top of the s band and bottom of the d band leading to a narrowing of the two subbands. Because of the degeneracies of the two bands the effect is most apparent in the s band. On increasing the separation between the atoms two things happen. The d and the s bands narrow and the interaction between them diminishes. The first effect causes $N(E_F)$ to increase, the second to decrease. Because the s-s interaction is longer range than the s-d interaction, $N(E_F)$ initially decreases and then increases montonically as the s-band narrowing eventually dominates. We can test to see if this is correct by performing a calculation where the Cs d states are omitted. This calculation is not self-consistent but is carried out with the potential from a fully self-consistent calculation where the d states were included. The resulting DOS for the bcc structure, $N_{sp}(E_F)$, is shown in Fig. 7 as a dashed line. At high densities it is more than a factor of 2 smaller than $N(E_F)$ with d's included, confirming that the d bands compress the s band. $N_{sp}(E_F)$ increases

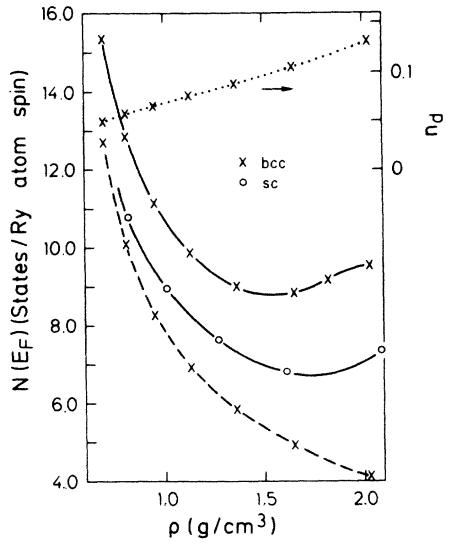

FIG. 7. $N(E_F)$ as a function of density for the bcc and sc structures. The dashed line is $N_{sp}(E_F)$, the density of states calculated without the d states. The dotted line is the number of d-like electrons in the occupied part of the band for the bcc structure.

monotonically with volume in agreement with the picture presented above. $N_{sp}(E_F)$ must asymptotically be equal to $N(E_F)$, but this only occurs at very low densities where there is no d-band mixing into the s band. This has not yet occurred, as can be seen by looking at n_d, the number of d-like electrons in the s band also shown in Fig. 7. Additional support for this interpretation is given by the absence of a minimum in the mass susceptibility of Na which has no nearby d bands.[7]

B. Ferromagnetism versus antiferromagnetism

From an analysis of the nuclear spin-lattice relaxation time due to the hyperfine interaction with the conduction electrons, El-Hanany *et al.*[5] concluded that at low densities there were changes in the wave-vector dependence of the low-frequency susceptibility $\chi(\mathbf{q},\omega)$ consistent with the onset of a spin-density wave. Bottyan *et al.*[7] found similar behavior for Na. The onset of magnetism is intimately connected with the M-I transition. In the low-density limit a lattice of one-electron atoms forms an AF insulator, while at high densities it is a paramagnetic metal. The situation in between is not clear. Recent local-density calculations[12,13,15] for a bcc hydrogen lattice find the sequence nonmagnetic metal→AF metal→AF insulator as the density is decreased. This is in agreement with Cyrot's solution[30] of Hubbards model for correlation in which emphasis is placed on the Coulomb repulsion between electrons on the same site.

In Fig. 9 the results of calculations of the static suceptibility $\chi(\mathbf{q})$ for bcc hydrogen[15] are shown for $\mathbf{q}=(0,0,0)$ (uniform susceptibility, χ_F) and the zone-boundary wave vector $\mathbf{q}=(2\pi/a)(1,0,0)$ (χ_{AF}). AF ordering occurs at $R_s=2.46$ and F ordering at $R_s=2.86$. For all but the highest densities ($R_s<1.7$) χ_{AF} is larger than χ_F. The AF state has lower energy than the F state for all densities.

In this section we describe the results of similar calculations for Cs. However, rather than calculate the susceptibility which can be very time consuming, we simply determine the density at which magnetic ordering occurs. The uniform susceptibility is given by Eq. (2) and shown in Fig. 4. We note that the criterion set by Eq. (2) for the onset of ferromagnetism, $N(E_F)I=1$, underestimates the density at which ordering occurs since it assumes a continuous onset. It frequently happens that the transition is first order and is determined by structure in the density of states.[15] A more general condition[24,25] for the onset of ferromagnetic ordering is that $\bar{N}(m)I=1$ where $\bar{N}(m)$ is the nonmagnetic DOS averaged over the exchange splitting. In terms of $E(n)$, the inverse of the number of states function

$$n(E)=\int_0^E N(E')dE' , \tag{4}$$

$$\bar{N}(m)=\frac{m}{E[(n+m)/2]-E[(n-m)/2]} , \tag{5}$$

where n is the number of conduction electrons. $E_F=E(n/2)$ and $\bar{N}(0)\equiv N(E_F)$. For bcc or sc Cs with one atom per unit cell, $n=1$; for the diamond structure there are two atoms per unit cell and $n=2$. $\bar{N}(n)=1/W$ so that the system becomes fully spin polarized when the

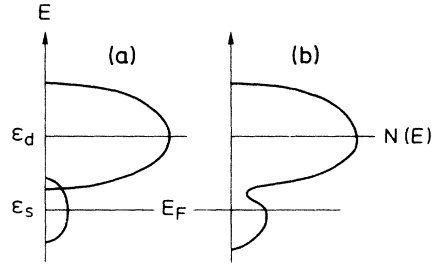

FIG. 8. Schematic DOS to illustrate the initial decrease in $N(E_F)$ for the bcc and sc structures. s and d DOS centered at ε_s and ε_d, respectively, where there is (a) no s-d interaction and (b) with s-d interaction switched on.

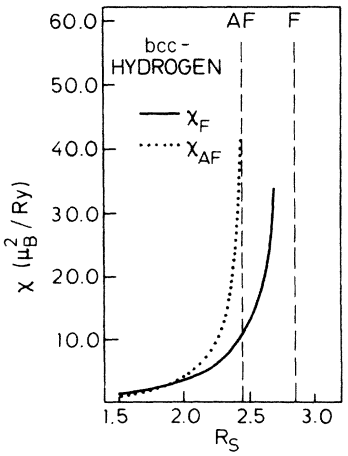

FIG. 9. Response of a bcc lattice of hydrogen atoms to a constant (χ_F) and staggered (χ_{AF}) external magnetic field as a function of volume. The vertical dashed lines indicate the F and AF onsets.

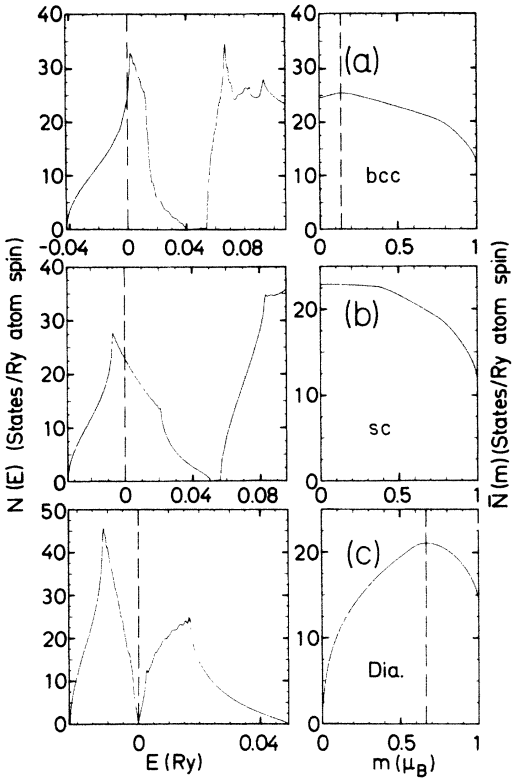

FIG. 10. Densities of states $N(E)$ and their corresponding $\bar{N}(m)$ functions calculated according to Eq. (5) for (a) bcc, (b) sc, and (c) diamond structures. $N(E)$ was calculated at a density close to the ferromagnetic onset for each particular structure.

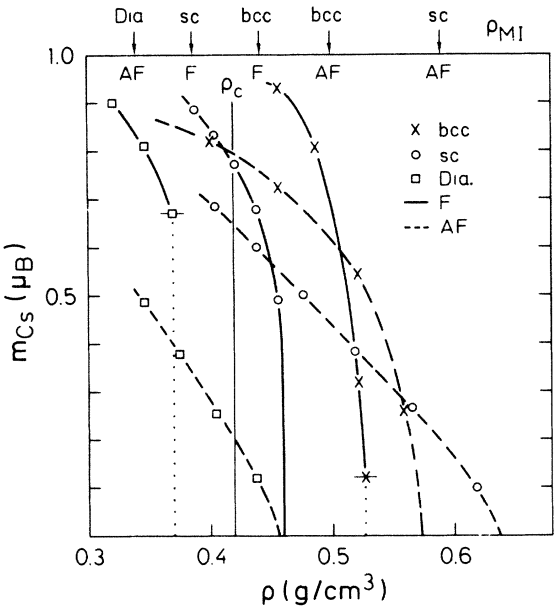

FIG. 11. Magnetic moment per Cs atom as a function of density for the bcc, sc, and diamond structures with F (solid line) and AF (dashed line) ordering. The densities at which the metal-insulator transition occurs, ρ_{MI}, is indicated by vertical arrows.

bandwidth is less than or equal to the exchange splitting.

The total densities of states for the bcc, sc, and diamond structures at densities close to those at which ferromagnetic ordering occurs are shown in Fig. 10 together with the corresponding $\bar{N}(m)$ functions calculated according to Eq. (5). There is a discontinuous transition for both the bcc and diamond structures. In the former case the magnetic moment at the onset, m_o, is $0.14\mu_B$; in the latter it is $0.67\mu_B$. The reason for the very large value of m_o for the diamond structure lies in the double-peak structure in the paramagnetic DOS where the Fermi level lies in a region of near-zero state density between the bonding and antibonding bands. For the sc structure the onset of ferromagnetism is continuous.

The evolution of the magnetic moments is shown in Fig. 11 for both F and AF ordering. For F ordering it is mainly determined by $\bar{N}(m)$. For AF ordering the moment changes continuously with density. We refer to Ref. 15 for a detailed discussion of the mechanisms driving the transitions.

In contrast to Rose,[14] who found that the magnetic and M-I transitions occurred at the same density, we find that the M-I transition occurs at a lower density. We believe the difference is due to computational simplifications made in Ref. 14.

For all three structures antiferromagnetism occurs before ferromagnetic ordering. The sequence for F ordering is bcc, sc, diamond as determined principally by $N(E_F)$. In our calculations for hydrogen[15] we found no evidence for Fermi-surface nesting, and, in general, AF ordering for itinerant antiferromagnets is not driven by Fermi-surface effects. For the onset of AF order we find the sequence NaCl, CsCl, ZnS. As the density decreases there are two contributions to the change in magnetic moment namely (i) loss of free Fermi surface and (ii) change in hybridization. At some density a transition occurs from an AF metal (AFM) to AF insulator (AFI). In the AFI phase only mechanism (ii) contributes to the change in moment, which increases only asymptotically to the atomic limit, in contrast to the F case where the system becomes fully spin polarized at the M-I transitions. In Fig. 11 the density at which a M-I transition occurs is indicated by a vertical arrow. For a given structure the transition from AFM→AFI occurs before the FM→FI transition and at densities clustered about the critical density. However, the gaps formed are smeared out by thermal excitations so that the M-I transitions in this model would occur at lower densities. In the LSD approximation the asymptotic value for the gap is $\varepsilon_{5s}^{\uparrow}-\varepsilon_{5s}^{\downarrow}$ where $\varepsilon^{\uparrow(\downarrow)}$ is the atomic eigenvalue from a spin-polarized calculation. For Cs it is 54 mRy. This is smaller than the correct SDF gap which is underestimated in the local approximation. For comparison T_c for cesium is 1740°C.[2]

For all three structures, bcc, sc, and diamond, the AF ordered phase has the lowest energy as has been found for bcc hydrogen.[12,15] However, the difference in energy between the AF and F phases is approximately 1 mRy/atom compared to ~12 mRy/atom found for hydrogen. The difference in energy between the nonmagnetic and magnetic phases is much larger, and in the atomic limit the energy of the spin-polarized atom is 11 mRy lower.

We do not expect any significant differences in the volume dependence of χ_{AF} for hydrogen and cesium. The AF ordering we have considered is the simplest possible for the bcc, sc, and diamond structures involving a doubling of the unit cell and no loss of point-group symmetry. It is of course possible to consider different magnetic order corresponding to larger super cells with lower point-group symmetry. The density at which we have found AF ordering to occur is, in general, a lower limit for the density at which an AF instability with some other q vector occurs. The same must be true also for the susceptibility so that we expect an enhancement of χ_{AF}/χ_F with decreasing density of the form found by El-Hanany *et al.*[5] and Bottyan *et al.*[7]

C. $\langle |\psi(0)|^2\rangle_{E_F}$

The Fermi electron probability density at the nucleus, $\langle |\psi(0)|^2\rangle_{E_F}$, normalized to the atomic $6s$ charge density at the nucleus $|\psi(0)|^2_{6s}$ and denoted ξ, was calculated according to Eq. (1) and is shown in Fig. 12. Also shown is the experimental value of ξ from Ref. 18. It has a roughly constant value of 0.51 from ρ_m down to $\rho \sim 1.4$ g/cm^3 where it starts to decrease. At the lowest measured density, $\rho \sim 1.0$ g/cm^3, it has a value of about 0.32. This behavior is contrary to a simple intuitive model by which we might expect ξ to increase towards the asymptotic atomic limit of 1 with decreasing density.

The calculated values of ξ for the sequence bcc-sc-diamond structures with constant $d_{NN}=10.03$ a.u. are joined by a dotted line in Fig. 12. It increases monotonically from a value of 0.68 (bcc) at $\rho=1.92$ g/cm^3 in agreement with the theoretical finding of Ref. 18. The high-density value is about 35% larger than the experimental value which is largely due to the uncertainty in the paramagnetic susceptibility. If we use the de Haas–van Alphen value of the susceptibility at high densities then the corresponding experimental value of ξ increases to 0.64. We note that the absolute values of the theoretical $\langle |\psi(0)|^2\rangle_{E_F}$ and $|\psi(0)|^2_{\text{atom}}$ contain a substantial error of uncertain origin.[31]

The volume dependence of ξ for each of the three structures studied is also shown in Fig. 12. Towards lower densities ξ_{bcc}, ξ_{sc}, and ξ_{dia} individually increase. At higher densities ξ_{bcc} initially decreases but then flattens out and increases towards the atomic limit. The separate components of $\langle |\psi(0)|^2\rangle_{E_F}$ in Eq. (1), $N_s(E_F)/N(E_F)$ and $\phi_s^2(E_F,0)$, are shown in Fig. 13. $N_s(E_F)/N(E_F)$ increases monotonically towards the atomic limit of 1. $\phi^2(E_F,0)$ decreases with decreasing density and has almost reached its asymptotic value at a value of ρ of 1.0 g/cm^3 where $N_s(E_F)/N(E_F)$ has started to increase rapidly. This then gives rise to the nonmonotonic behavior of ξ_{bcc}.

The shaded area represents the energy dependence of $\phi^2(E,0)$ between the bottom, $E_B=E_F-W/2$, and top, $E_T=E_F+W/2$ of the cesium s band and is roughly constant over the density range shown. $\phi^2(E,0)$ increases from the bottom to the top of the band. The reason is simple and is illustrated in the inset to Fig. 13. At the bottom of the band the bonding wave function has a maximum between the atoms. Because $\phi^2(E,r)$ is normalized

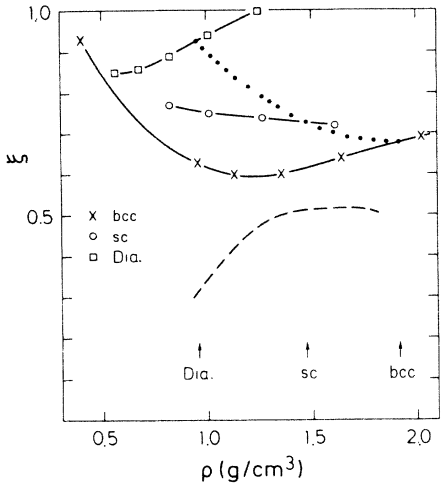

FIG. 12. Density dependence of ξ calculated for the bcc, sc, and diamond structures. The dashed line is the experimental ξ from Ref. 18. The dotted line corresponds to the sequence bcc-sc-diamond with $d_{NN}=10.03$ a.u.

to 1 inside the Wigner-Seitz atomic sphere its value at the nucleus is reduced.

Similarly the antibonding wave function which has zero amplitude between atoms is renormalized so that $\phi^2(E_T,0)$ is large. This suggests a possibility to explain the decrease in ξ with decreasing density. The occurrence of dimerization with the formation of a bond between neighboring pairs of Cs atoms could lead to a reduced $\phi^2(E_F,0)$. There is evidence for the existence of Cs_2 molecules in the dense vapor phase which has been discussed by Freyland.[3]

To investigate the effect of pairing we consider dimer-

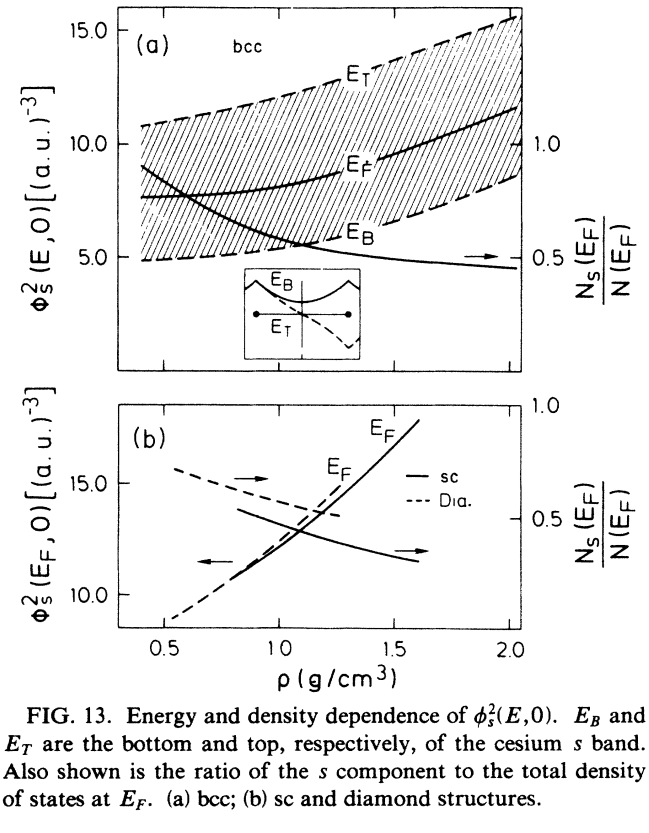

FIG. 13. Energy and density dependence of $\phi_s^2(E,0)$. E_B and E_T are the bottom and top, respectively, of the cesium s band. Also shown is the ratio of the s component to the total density of states at E_F. (a) bcc; (b) sc and diamond structures.

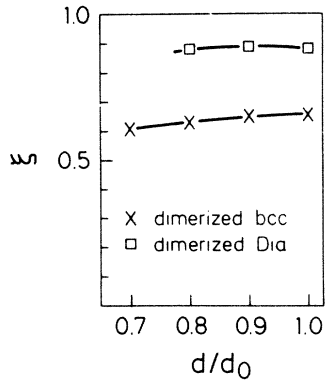

FIG. 14. ξ for the dimerized bcc and diamond structures described in the text as a function of the dimer spacing $d \equiv d_{NN}$. $\rho_{bcc}=0.81$ g/cm^3 and $\rho_{dia}=0.82$ g/cm^3.

ized bcc and diamond structures. At a density of 0.8 g/cm^3, $d_{NN}^{CsCl}=13.4$ a.u. and $d_{NN}^{ZnS}=10.6$ a.u. For comparison, d_{NN} for crystalline Cs at normal pressure is 9.9 a.u., for the liquid metal it is 10.0 a.u., and for the $^1\Sigma_g^+$ ground state of the Cs_2 molecule it is 8.5 a.u.

The dimerized bcc structure we consider has a simple cubic Bravais lattice with atoms at (0,0,0) and $(a/2)(q,q,q)$. The dimerized diamond structure has a fcc Bravais lattice with a basis (0,0,0) and $(a/4)(q,q,q)$. For $q=1$ we recover the bcc and diamond structures.

The results of these calculations of ξ as a function of d_{NN} are shown in Fig. 14. The densities for the bcc and diamond structures shown were 0.81 and 0.82 g/cm^3, respectively. For the diamond structure ξ is not altered by the dimerization. For the bcc structure ξ indeed decreases as the atoms pair, but the decrease is much too small to account for experiment. In addition, it is driven by a decrease in $N(E_F)$ [$\phi_s^2(E_F,0)$ increases slightly] which would imply an even smaller enhancement of the static susceptibility for the paired structure. We conclude that the reduction of ξ with decreasing density is not driven by a simple pairing of Cs atoms.

IV. CONCLUSIONS

We have explored the density-functional description of low-density metallic cesium within the local-spin-density approximation and assuming a simple structural model for the expanded liquid. This simple mean-field theory predicts the onset of a spin-density wave at a density above the critical density ρ_c and a corresponding enhancement of $\chi(\mathbf{q})$ for some finite wave vector at higher densities. This is in agreement with experiment. However, the calculations for bcc, sc, and diamond structures fail to reproduce the observed strong enhancement of the uniform static susceptibility and the decrease in $\langle |\psi(0)|^2\rangle_{E_F}$ at low densities. While alternative structures with coordination number $z\sim 4$ may exist which have a large $N(E_F)$, such DOS features are unlikely to survive at the high temperatures required to attain the density of $\rho\sim 0.8$ g/cm^3. The decrease in bandwidth alone was insufficient to yield the observed enhancement.

For low-density hydrogen we have found[15] that the onset of antiferromagnetism does not appreciably alter the uniform static susceptibility. For cesium the AF onset occurs at densities between 0.64 and 0.46 g/cm^3 (depending on the structure) and does not affect the uniform susceptibility or $\langle |\psi(0)|^2\rangle_{E_F}$ at higher densities.

We examined the effect of dimerization on $\langle |\psi(0)|^2\rangle_{E_F}$, but found that it did not lead to a significant reduction in ξ. Since the ground state of the Cs_2 molecule is a singlet, objections might be made that the appropriate dimerized structure should be AF. However, exploratory calculations[32] at $\rho=0.8$ g/cm^3 indicate that the dimerized structure does not become AF at this density.

The reason for the failure of the model to describe the low-density electronic properties is not clear. Inclusion of temperature in a simplistic fashion[24] would only further reduce the calculated enhancement. An alternative structural model for expanded liquid cesium proposed by Franz[16] stresses the effect of disorder while maintaining the feature of a fixed nearest-neighbor separation d_{NN}. It is, however, difficult to evaluate this model quantitatively because of the many approximations made in implementing it. While it is, in principle, possible to examine this model within the local-density approximation, this is not at present feasible.

ACKNOWLEDGMENTS

We are grateful to T. M. Rice for suggesting this research project and to O. K. Andersen for a critical reading of the manuscript. One of us (P.J.K.) is also grateful for discussions with W. W. Warren and J. H. Rose.

*Present address: Philips Research Laboratories, P. O. Box 80.000, 5600 JA Eindhoven, The Netherlands.

[1]N. F. Mott. Proc. Phys. Soc. London, Sect. A **62**, 416 (1949).

[2]G. Franz, W. Freyland, and F. Hensel, J. Phys. (Paris) Colloq. **41**, C8-70 (1980).

[3]W. Freyland, Phys. Rev. B **20**, 5104 (1979).

[4]W. W. Warren, Jr., Phys. Rev. B **29**, 7012 (1984).

[5]U. El-Hanany, G. F. Brennert, and W. W. Warren, Jr., Phys. Rev. Lett. **50**, 540 (1983).

[6]W. W. Warren, Jr., U. El-Hanany, and G. F. Brennert, Proceedings of the Fifth International Conference on Liquid and Amorphous Metals [J. Non-Crystalline Solids **61-62**, 23 (1984)].

[7]L. Bottyan, R. Dupree, and W. Freyland, J. Phys. F **13**, L173 (1983).

[8]P. Hohenberg and W. Kohn, Phys. Rev. **136**, B864 (1964); W. Kohn and L. J. Sham, *ibid.* **140**, A1133 (1965).

[9]For a recent review of applications of density-functional theory, see U. von Barth and A. R. Williams, in *Theory of the Inhomogeneous Electron Gas,* edited by S. Lundqvist and N.

H. March (Plenum, New York, 1983).
[10]U. von Barth and L. Hedin, J. Phys. C **5**, 1629 (1972).
[11]O. Gunnarsson and B. I. Lundqvist, Phys. Rev. B **13**, 4274 (1976).
[12]L. M. Sander, H. B. Shore, and J. H. Rose, Phys. Rev. B **24**, 4879 (1981).
[13]J. H. Rose, H. B. Shore, and L. M. Sander, Phys. Rev. B **21**, 3037 (1980).
[14]J. H. Rose, Phys. Rev. B **23**, 552 (1981).
[15]P. J. Kelly, O. K. Andersen, and T. M. Rice (unpublished).
[16]J. R. Franz, Phys. Rev. B **29**, 1565 (1984).
[17]G. Franz, W. Freyland, W. Gläser, F. Hensel, and E. Schneider, J. Phys. (Paris) Colloq. **41**, C8-194 (1980).
[18]W. W. Warren, Jr. and L. F. Mattheiss, Phys. Rev. B **30**, 3103 (1984).
[19]O. K. Andersen, Phys. Rev. B **12**, 3060 (1975).
[20]D. D. Koelling and B. N. Harmon, J. Phys. C **10**, 3107 (1977).
[21]O. Jepsen and O. K. Andersen, Solid State Commun. **9**, 1763 (1971); G. Lehmann and M. Taut, Phys. Status Solidi B **54**, 469 (1972).
[22]See, for example, D. Glötzel, B. Segall, and O. K. Andersen, Solid State Commun. **36**, 403 (1980).
[23]T. Asada and K. Terakura, J. Phys. F **13**, 799 (1983).
[24]O. Gunnarsson, J. Phys. F **6**, 587 (1976).
[25]O. K. Andersen, J. Madsen, U. K. Poulsen, O. Jepsen, and J. Kollar, Physica **86-88B**, 249 (1977).
[26]S. H. Vosko and J. P. Perdew, Can. J. Phys. **53**, 1385 (1975); S. H. Vosko, J. P. Perdew, and A. H. MacDonald, Phys. Rev. Lett. **35**, 1725 (1975).
[27]J. F. Janak, Phys. Rev. B **16**, 255 (1977).
[28]J. P. Jan, A. H. MacDonald, and H. L. Skriver, Phys. Rev. B **21**, 5584 (1980).
[29]N. S. Gingrich and L. Heaton, J. Chem. Phys. **34**, 873 (1961).
[30]M. Cyrot, Philos. Mag. **25**, 1031 (1972).
[31]See H. Chermette, Phys. Rev. A **29**, 488 (1984), for a recent discussion of relativistic and core-polarization effects as well as for a comparison of $X\alpha$ and LSD approximations for free alkali atoms. The effect of including core polarization in a LSD calculation of the Knight shift of the alkaline earth and alkali metals is discussed in E. Zaremba and D. Zobin, Phys. Rev. Lett. **44**, 175 (1980).
[32]P. J. Kelly (unpublished).